Three-Dimensional Cloud Characterization from Paired Whole-Sky Imaging Cameras

M. Allmen and W. P. Kegelmeyer, Jr.
Sandia National Laboratories
Livermore, CA 94551

Three-dimensional (3-D) cloud characterization permits the derivation of important cloud geometry properties such as fractional cloudiness, mean cloud and clear length, aspect ratio, and the morphology of cloud cover. These properties are needed as input to the hierarchical diagnosis (HD) and instantaneous radiative transfer (IRF) models, to validate sub-models for cloud occurrence and formation, and to Central Site radiative flux calculations. A full 3-D characterization will eventually require the integration of disparate Cloud and Radiation Testbed (CART) data sources: whole-sky imagers (WSIs), radar, satellites, ceilometers, volume-imaging lidar, and other sensors. In this paper, we demonstrate how an initial 3-D cloud property, cloud base height, can be determined from fusing paired time series of images from two whole-sky imagers.

Background

GCMs and Clouds

A major goal for the Department of Energy's (DOE's) global change efforts is to improve the accuracy of general circulation models (GCMs) capable of predicting the timing and magnitude of greenhouse-gas-induced global warming. Research has shown cloud radiative feedback is the single most important feedback effect determining the magnitude of possible climate responses to human activity. Yet, as pointed out by Cess et al. (1989), clouds are not well parameterized in GCMs and are, in fact, currently the greatest factor limiting the accuracy of atmospheric GCMs. Thus clouds exert the largest influence while at the same time present the largest uncertainties in predicting global climate change. As a result, cloud studies are critical to understanding global climate change and improving the predictive accuracy of GCMs. In recognition of this problem, a number of important national and international programs (Rossow et al. 1985) have been initiated to characterize cloud-radiation interactions, including DOE's Atmospheric Radiation Measurement (ARM) Program and the International Satellite Cloud Climatology Project (ISCCP).

In the ARM Program, a key to characterizing cloud-radiation interactions is the effective treatment of cloud formation and cloud properties in GCMs as supported by a field measurements program—"an important feature of the ARM Program Plan is to establish a surface-based cloud imaging system at the research sites that will provide appropriate information for parameterizing solar flux over an entire grid cell." The first such Cloud and Radiation Testbed (CART) site will make measurements, including cloud measurements, over a 30-km diameter region.

Macroscopic Cloud Properties

A well-recognized approach to reducing the uncertainties associated with cloud-radiation interactions involves measuring the macroscopic properties of clouds (shape, size, extent, cloud cover fraction, base height, etc.). All these properties can be extracted from a 3-D cloud characterization, and so the development of such a characterization is a worthy goal. Accordingly, we have been studying methods for atmospheric data integration, beginning with fusing WSI imagery to determine cloud base height. This property is a good place to start in that it is a dominant factor in determining the infrared radiation from clouds to the lower atmosphere and the earth's surface. Furthermore, as shown by Rossow et al. (1985), base heights are essential to measuring the cloud cover fraction at low, medium and high altitude, measurements that, in turn, are needed to establish a cloud-radiation climatology.

Whole Sky Imagers

Digital whole-sky imagers have a number of advantages for making cloud studies. They are passive and therefore relatively inexpensive and reliable, can be used in unattended operation, and can obtain images of the entire sky dome rapidly. The particular camera which generated our existing data is the Whole Sky Imager developed by the Marine Physical Laboratory (MPL) at the Scripps Institution of Oceanography, as described in Shields et al. (1990). These imagers are rugged and have demonstrated many years of high-reliability field service. Full-resolution (1/3 degrees) digital images can be acquired at one per minute. This is rapid enough to capture most of the cloud dynamics of interest and fully exploit the image motion of the clouds as an aid in 3-D analysis, as described below.

Method

An Overview

Unfortunately, the state of the art in automatic cloud imagery processing was not previously capable of extracting measures as central and important as cloud bottom heights over large regions of the sky dome. The main difficulty is spatially matching up cloud fields from widely separated WSI cameras. However, once correctly registered against each other, computation of cloud bottom heights proceeds in a straightforward fashion from triangulation and knowledge of the camera locations. Our solution to this problem (initially reported in Allmen and Kegelmeyer (1993), on which this report builds) utilizes temporal flow fields from each camera separately. In the following subsections we will review the prior history of this problem, illustrate its difficulty, and suggest why flow fields provide the additional information necessary to make this problem solvable.

Prior Work

Extracting cloud bottom heights via triangulation of registered points has been in the cloud stereoscopy literature for twenty years and is well-understood. The registration itself, however, has not been well addressed. In the earlier literature, e.g., Bradbury and Fujita (1968) and Lyons(1971), the problem was side-stepped though human intervention: the images were registered by hand before triangulation. More recently, e.g., Rock (1987), the automatic registration problem has been successfully handled, but only for nearly adjacent views of the sky, which limits to a small fraction of the sky dome the region over which the analysis can be performed. In such a case, the stereoscopic nature of the views permitted simple limited-displacement correlation to suffice as a registration algorithm.

The registration problem facing ARM, however, is considerably harder in that the camera spacing will be on the order of 5 km. This spacing is required to achieve adequate coverage at the required resolution with a small number of cameras. With this baseline spacing, the 3-D nature of clouds generates occlusion and perspective effects that will cause them to image differently at the various cameras. Because of this, correlation-based registration using pixel intensity alone will fail. Further, the visual self-similarity of clouds will defeat token matching (the detection and matching of a small number of visually distinctive regions), which is the only common alternative approach.

As an example, the top of Figure 1 contains an example pair of synthetic simultaneous frames (see the next section for how the data were generated). Careful examination will show that corresponding points appear shifted to the left in the right image. This shift can be difficult to determine by eye, primarily because of the difference in perspective experienced by the widely separated cameras. Finding corresponding points in WSI images of real-world cloud fields is even more challenging, creating the need to also use flow fields to find corresponding points.

Flow Field Correlation

The use of image sequences to identify the correspondence suggests how one can automate the registration process. WSI images are acquired at a rate of one per minute, which provides a comparatively dynamic view of the sky. This provides a means to overcome the registration obstacles mentioned before, which apply only to the attempt to register two static views of the sky.

The temporal sampling rate of the WSI camera is high enough that optical flow fields can be computed using hierarchical correlation methods such as those developed by Burt (1984). With the optical flow fields computed for the

images from both WSI cameras, each image pixel becomes associated with a vector indicating the image motion of that point. Combining this with the intensity value at the pixel, a three-dimensional quantity now represents each image pixel. The core of our approach is to jointly register the flow and intensity fields from the separated WSIs against each other. In this way, the additional constraints provided by the flow field are exploited to make the matching unique.

The Test Data and Results

We have computed cloud base heights from various synthetic image sequences and from real WSI data collected under conditions designed to simulate those of the CART site.

Simulated Data

The simulated sequences were created with a cloud scene simulation model developed by Cianciolo (1992). The model uses stochastic field generation techniques and knowledge of atmospheric structure and physics to model four-dimensional (3 spatial and 1 temporal) cloud scenes, represented by liquid water content (LWC) values. To this, we attached a cloud density model to derive radiance fields from the LWC volumes. Synthetic images were then generated by projecting a cloud scene using a WSI camera model that is identical to an actual WSI. Since the cloud scene has a temporal component, it can be projected at a sequence of times, creating an image sequence that captures cloud evolution and motion. This allows calculation and, most importantly, verification of cloud base heights on realistic data. Moreover, the simulation can produce a wider range of cloud types than exists in our real imagery.

The top of Figure 1 shows one frame from the left and right image sequence of an altostratus cloud layer. In both cases the images depict a common cloud field as imaged from a horizontally paired set of WSI cameras, where black indicates sky and the mottled dark texture is cloud. The cameras were modeled as being separated by 5 km, and the clouds were set at heights between 3 and 5 km.

Careful examination reveals that the corresponding points appear shifted to the left in the right image. This is difficult to note from simple inspection, primarily because of the difference in perspective experienced by the widely separated cameras.

Simulated Data Results

The fact that the data are simulated and that we thus know the true cloud height at every point means that we can evaluate the accuracy of the algorithm on a pixel-by-pixel basis.

Some results for the simulated altostratus sequence are presented in the bottom of Figure 1. One of the innovative features of our algorithm is that at each pixel it provides a *confidence* measure that it has computed the correct height. The bottom left image illustrates, via the middle grey level, the points where the algorithm was confident it had computed the correct height and in fact was correct (within 5%). The white points are where the algorithm erroneously computed the heights as being too high, black is where it erroneously computed the heights as being too low, and the rest is background or points where the algorithm evaluated itself as likely to be erroneous and so did not hazard a guess.

Clearly, the number of correct points is far greater than the number of incorrect points. To make this quantitative, the bottom right part of Figure 1 shows the histogram of the errors for the points where the algorithm was confident. The desired result is a sharp peak at zero error; the histogram here has a bin size of 200 m and so demonstrates that 84% of the confidently computed heights were accurate.

Real Data

Our real WSI data were taken in May 1992 in White Sands, NM. In an attempt to simulate the eventual CART data, we separated two WSIs by 5.54 km, with a ceilometer located close to the midpoint between them. The intent of the ceilometer was to provide fiduciary points with which to check our algorithm. It was fired once a minute, in time with both WSIs. As a result, when the ceilometer reports the presence of clouds, simple geometry and knowledge of the camera location suffice to compute which pixel on the WSI images corresponds to that ceilometer report. The cloud base height computed at that point can then be compared to the ceilometer measurement.

The top two images in Figure 2 are examples of these real WSI images from mid-day on May 4. The inset white circle indicates the location of the ceilometer hit on both images.

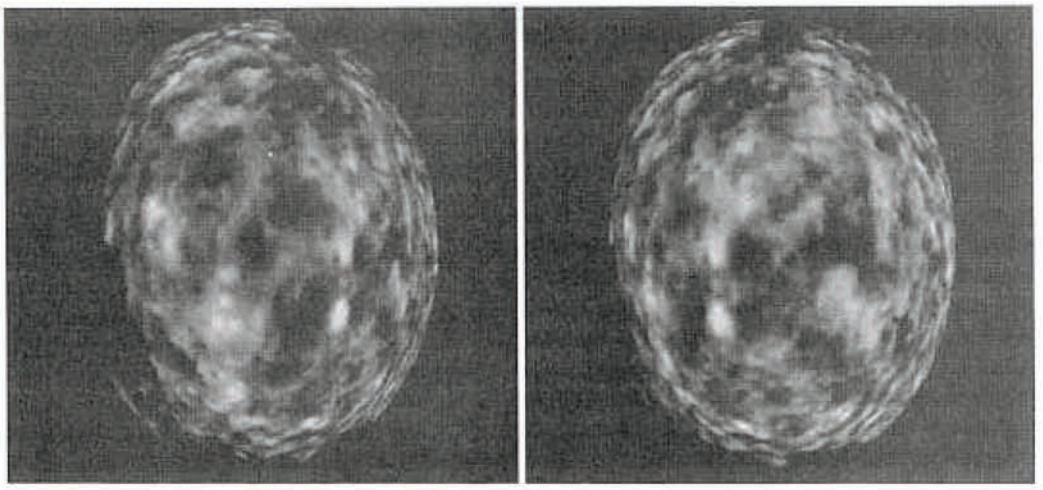

(a) Simulated Altostratus, Left Image

(b) Simulated Altostratus, Right Image

(c) Height Correctness for Left Image

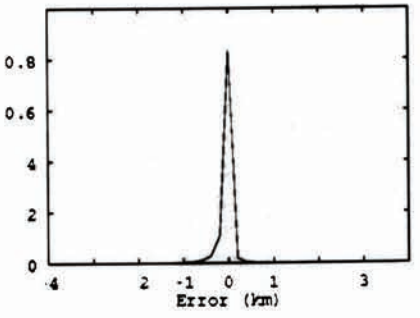

(d) Error Histogram for Left Image

Figure 1. One frame of an altostratus cloud scene as viewed from the left (top left image) and right (top right image) cameras. The bottom left image illustrates, via the middle grey level, the points where the algorithm was confident it had computed the correct height and, in fact, was correct (within 5%). The white points are where the algorithm erroneously computed the heights as being too high, black is where it erroneously computed the heights as being too low, and the rest is background or points where the algorithm evaluated itself as likely to be erroneous and so did not make a report. The bottom right image shows a histogram of the error in height computation.

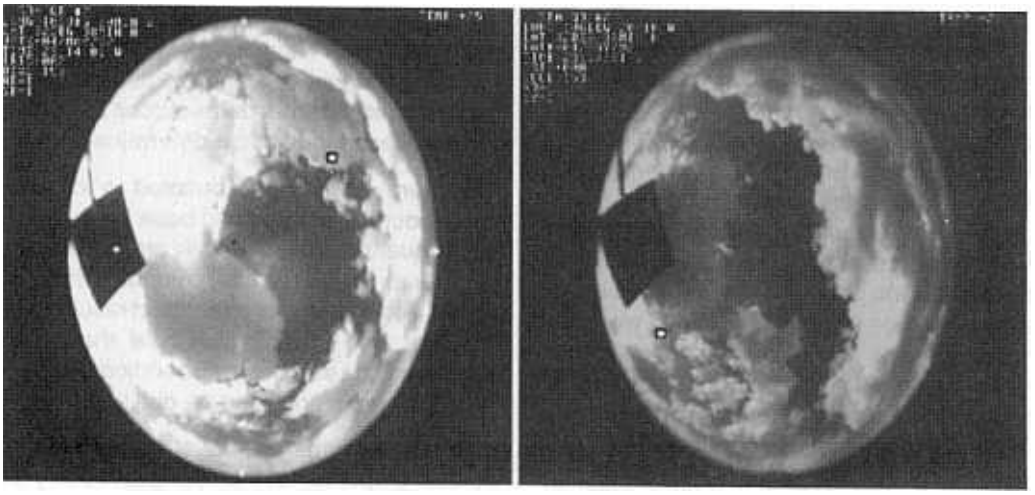

(a) Real WSI, Left Image

(b) Real WSI, Right Image

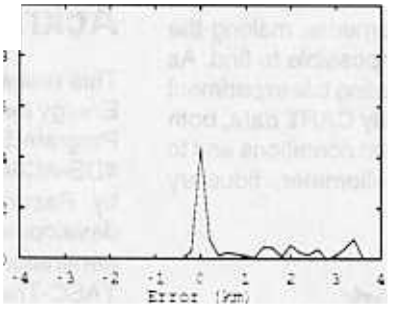

(c) Error Histogram for Entire Day

Figure 2. One frame of a real cloud scene as viewed from the left (top left image)and right (top right image) cameras. The bottom image shows a histogram of height error as calculated from a ceilometer over the course of a day.

Real Data Results

Since we do not know the true cloud base height at every point, a height correctness image such as in the lower left of Figure 1 is not possible. For each frame, we know the ceilometer's height measurement for only a single point, not over the entire field of view. So the error histogram in the bottom of Figure 2 represents statistics extracted from the entire day. The peak of the histogram here is lower than for the simulated data. One straightforward reason is that the ceilometer had a range of only 4 km. Thus we could gather statistics only on the lower clouds, and low clouds are the worst case scenario for this approach, as the visual disparity of corresponding points is greatest. The algorithm improves in accuracy as the clouds get higher.

More significantly, we are concerned that our ceilometer data are not entirely reliable, as there are many cases where the ceilometer reports the presence or absence of a cloud in direct contradiction of the matching WSI image. We have recently become aware of the possibility of errors in our current camera calibration parameters as well, which would at times induce displacements, making the correct point registration difficult or impossible to find. As a result, we are looking forward to replicating this experiment with firmly documented and high quality CART data, both in order to span a broader range of cloud conditions and to have, from radar and long-range ceilometer, fiduciary points at higher altitudes.

Conclusions and Future Work

In summary, we began with a discussion of the value of 3-D cloud characterization to ARM's needs and suggested that such a characterization will require the fusion of many data sources from a rich suite that will be available at the CART sites. We have illustrated this principle with a demonstration of how paired data from widely separated whole-sky imager scan be fused to extract cloud base heights, an important cloud property and one which could not be recovered from either imager alone. An important feature of our approach, one that will help it to generalize to the incorporation of other data sources, is its ability to measure its own confidence in the determined base heights.

Near-term work will be devoted to the understanding of error sources in the cloud base height algorithm, and its subsequent improvement. We are evaluating the application of spatial filtering to the computed heights, so that the small, isolated regions of incorrect results can be eliminated. We are also investigating how the parameters of the algorithm, the size of the correlation neighborhood around a point for example, can be optimized.

Our future efforts are devoted both to the extraction of further properties of interest (particularly fractional cloud cover and aspect ratio) from paired WSI images, and fusing of WSI images with satellite imagery in order to determine cloud top structure as well.

Acknowledgments

This research was supported by the U.S. Department of Energy through the Atmospheric Radiation Measurement Program, Sandia National Laboratories, Livermore, contract #DE-AC04-76DO00789. The Khoros[a] system, developed by Rasure and Williams (1991), was used for code development and digital image visualization. Code for the generation of synthetic cloud scenes was provided by TASC-The Analytic Sciences Corporation, and the code which simulates radiance maps and projects 3-D cloud volumes into simulated WSI imagery was written by Chen-Hui Sun of Sandia National Laboratories.

(a) A publicly available integrated software development environment for information processing and visualization. Send e-mail to *khoros@chama.eece.unm.edu* for further information.

References

Allmen, M., and W. P. Kegelmeyer, Jr. 1993. The computation of cloud base height from paired whole sky imaging cameras. In *Fourth Symposium on Global Change Studies*, pp. 136-141. American Meteorological Society. Boston, Massachusetts.

Bradbury, D. L., and T. Fujita. 1968. Computation of height and velocity of clouds from dual, whole-sky, time-lapse picture sequences. SMRP Research Paper 90, Department of the Geophysical Sciences, University of Chicago, Chicago.

Burt, P. J. 1984. The pyramid as a structure for efficient computation. In *Multiresolution Image Processing and Analysis*, ed. A. Rosenfeld, pp. 7-35. Springer, Berlin.

Cess, R., G. L. Potter, J. P. Blanchet, G. J. Boer, S. J. Ghan, J. T. Kiehl, H. Le Treut, Z.-X. Li, X.-Z. Liang, J. F. B. Mitchell, J.-J. Morcrette, D. A. Randall, M. R. Riches, E. Roeckler, U. Schlese, A. Slingo, K. E. Taylor, W. M. Washington, R. T. Wetherald, and I. Yagai. 1989. Interpretation of cloud-climate feedback as produced by 14 atmospheric general circulation models. *Science* **245**:513-516.

Cianciolo, M. E. 1992. *Cloud scene simulation modeling: The enhanced model—Final report.* Tech. Rep. TR-6042-2, TASC, 55 Walkers Brook Drive, Reading, Massachusetts, 01867.

Lyons, R. D. 1971. *Computation of height and velocity of clouds over Barbados from a whole-sky camera network.* SMRP Research Report 95, Department of Geophysical Sciences, University of Chicago, Chicago.

Rasure, J., and C. Williams. 1991. An integrated visual language and software development environment. *J. Visual Languages and Computing* **2**:217-246.

Rocks, J. K. 1987. *The whole sky sensor: Phase 1 final report.* DTIC AD-A179 271.

Rossow, W., F. Mosher, E. Kinsella, A. Arking, M. Desbois, E. Harrison, P. Minnis, E. Ruprecht, G. Seze, C. Simmer, and E. Smith. 1985. ISCCP cloud algorithm intercomparison. *J. Clim. Appl. Meteorol.* **29**(9):877.

Shields, J., T. Koehler, and M. Karr. 1990. Automated cloud cover and visibility systems for real time applications. Technical Note 217, Marine Physical Laboratory, Scripps Institution of Oceanography, San Diego, California, 92151-6400.